

# Charge fluctuation induced superconducting state in two-dimensional quarter-filled electron systems

Akito KOBAYASHI<sup>1)</sup>, Yasuhiro TANAKA<sup>2)</sup>, Masao OGATA<sup>2)</sup> and Yoshikazu SUZUMURA<sup>1)</sup>

*1)Department of Physics, Nagoya University, Nagoya 464-8602*

*2)Department of Physics, University of Tokyo, Hongo, Bunkyo-ku, Tokyo 113-0033*

We investigate the superconducting (SC) state in two-dimensional extended Hubbard model at a quarter-filling with the on-site repulsive interaction ( $U$ ) and the nearest-neighbor one ( $V$ ), which lead to the spin fluctuation and the charge fluctuation, respectively. The effect of the charge fluctuation on the onset of the SC state is calculated by estimating the pairing interaction within the random phase approximation. Solving the linearized Eliashberg equation with the anomalous self-energy as the function of both momentum and frequency, we examined the singlet SC state on the plane of  $U$  and  $V$  with the fixed temperature. We found a novel result that the SC state with the  $d_{xy}$  symmetry retains for most parameters of  $U$  and  $V$ , although the pairing interaction changes the sign from repulsive one into attractive one with increasing  $V$ . The reentrant transition as the function of temperature occurs close to the onset of the SC state.

KEYWORDS: d-wave superconducting state, spin fluctuation, charge fluctuation, nearest-neighbor repulsive interaction, extended Hubbard model

Organic conductors exhibit the variety of superconducting (SC) states, as found in quasi-one-dimensional (Q1D) materials of Bechgaard salts,<sup>1)</sup> or quasi-two-dimensional (Q2D) materials of ET salts.<sup>2,3)</sup> It has been often asserted that the spin fluctuation is the origin of the SC state since the spin density wave state is located next to the SC state in the phase diagram. However there are some ET salts suggesting another possibility that the charge fluctuation could be the origin of the SC state. In  $\theta$ -ET<sub>2</sub>X salts, where the dihedral angle between two adjacent molecules changes with the choices of the anion X, it has been shown that the state with the charge ordering moves into the SC state with decreasing the dihedral angle<sup>2)</sup> corresponding to the increase of transfer energy. It is noteworthy that this SC state is located besides the charge ordering state. Moreover there is the recent observation of the

SC state in the Q2D conductor,  $\beta'$ -ET<sub>2</sub>ICl<sub>2</sub>, which appears under the pressure of  $\sim 8$  GPa.<sup>4)</sup> This indicates the increase of the nearest-neighbor repulsive interaction in addition to the increase of the transfer energy.

In 2D systems, there are several theoretical work for the SC state, which is based on the FLEX ( fluctuation exchange ) approximation.<sup>5)</sup> Especially, the spin fluctuation as the origin of the singlet SC state has been calculated for several transfer energies. By using a model with the on-site repulsive interaction  $U$  and a variation from the square lattice to the triangular lattice,<sup>6)</sup> it has been shown that the SC state at half-filling is mainly determined by the state with the  $d_{x^2-y^2}$  symmetry. On the other hand, in the presence of the nearest neighbor repulsive interaction  $V$ , there appears the SC state with the  $d_{xy}$  symmetry due to the charge fluctuation, as shown by the RPA (random phase approximation)<sup>7)</sup> with a choice of  $U$  and  $V$  and by the slave-boson theory with a quarter-filled band.<sup>8)</sup> However, it is not yet clear how the interplay of  $U$  and  $V$  leads to a crossover from the spin fluctuation to the charge fluctuation especially for the quarter-filled band.

In the present paper, such a role of charge fluctuation is studied by using the two-dimensional extended Hubbard model at the quarter-filling of hole doping. The case of the square lattice is examined as the first step since the transfer integral in organic conductors is very complicated. Within RPA,<sup>9,10,7)</sup> we examine a phase diagram of SC, SDW (spin density wave) and CDW (charge density wave) on the plane of  $U$  and  $V$  and also these states as the function of temperature.

We consider the expended Hubbard model given by

$$H = \sum_{\mathbf{k}\sigma} \varepsilon_{\mathbf{k}} c_{\mathbf{k}\sigma}^{\dagger} c_{\mathbf{k}\sigma} + U \sum_i n_{i\uparrow} n_{i\downarrow} + V \sum_{\langle ij \rangle} n_i n_j , \quad (1)$$

where quantities  $U$  and  $V$  are the coupling constants for on-site and nearest-neighbor repulsive interactions. The quantity  $\varepsilon_{\mathbf{k}}$  denotes the band energy of the 2D square lattice,  $\varepsilon_{\mathbf{k}} = -2t(\cos k_x a + \cos k_y a) - \mu$ , where  $t$  is the nearest-neighbor transfer energy and  $\mu$  is determined to obtain the 3/4-filled band, i.e., 1/4-filled hole band. In eq. (1),  $N_L$  is the total number of the lattice site and  $a$  is the lattice constant. We set  $t = 1$ ,  $a = 1$  and  $k_B = 1$ .

First, we calculate spin and charge susceptibilities given by

$$\chi^A(\mathbf{q}, \omega_l) = \frac{1}{2N_L} \sum_{\mathbf{k}, \mathbf{k}', \sigma, \sigma'} \int_0^{1/T} d\tau f_{\sigma} f_{\sigma'} \langle T_{\tau} c_{\mathbf{k}+\mathbf{q}, \sigma}^{\dagger}(\tau) c_{\mathbf{k}, \sigma}(\tau) c_{\mathbf{k}', \sigma'}^{\dagger}(0) c_{\mathbf{k}'+\mathbf{q}, \sigma'}(0) \rangle e^{i\omega_l \tau} , \quad (2)$$

with  $T$  and  $T_{\tau}$  being the temperature and the time ordering operator of the imaginary time. The spin susceptibility is given by  $A = s$  and  $f_{\sigma} = 1 (= -1)$  for  $\sigma = \uparrow (= \downarrow)$  while the charge susceptibility is given by  $A = c$  and  $f_{\sigma} = 1$ . The irreducible susceptibility  $\chi^0(\mathbf{q}, \omega_l)$ , which

denotes eq.(2) without the interactions, is given by

$$\chi^0(\mathbf{q}, \omega_l) = -\frac{T}{N_L} \sum_{\mathbf{k}, m} G^0(\mathbf{k} + \mathbf{q}, \epsilon_m + \omega_l) G^0(\mathbf{k}, \epsilon_m) , \quad (3)$$

where  $\omega_l$  ( $\epsilon_m$ ) is the Matsubara frequency for boson (fermion) and  $G^0(\mathbf{k}, \epsilon_m) = [i\epsilon_m - \epsilon_{\mathbf{k}}]^{-1}$ . Treating  $U$  and  $V$  terms of eq. (1) within RPA, eq.(2) is calculated as

$$\chi^s(\mathbf{q}, \omega_l) = \chi^0(\mathbf{q}, \omega_l) / (1 - U\chi^0(\mathbf{q}, \omega_l)) , \quad (4)$$

$$\chi^c(\mathbf{q}, \omega_l) = \chi^0(\mathbf{q}, \omega_l) / (1 + (U + 2V(\mathbf{q}))\chi^0(\mathbf{q}, \omega_l)) , \quad (5)$$

where  $V(\mathbf{q}) = 2V(\cos q_x a + \cos q_y a)$ .

Next, we derive the pairing interaction,  $P(\mathbf{q}, \omega_l)$ , corresponding to the vertex for the singlet state

$$P(\mathbf{q}, \omega_l) \int_0^{1/T} d\tau c_{\mathbf{k}-\mathbf{q}, \uparrow}^\dagger(\tau) c_{-\mathbf{k}+\mathbf{q}, \downarrow}^\dagger(\tau) c_{-\mathbf{k}, \downarrow}(0) c_{\mathbf{k}, \uparrow}(0) e^{i\omega_l \tau} , \quad (6)$$

which is used in the Eliashberg equation for the SC state. In terms of eqs. (4) and (5), the pairing interaction  $P(\mathbf{q}, \omega_l)$  is obtained as

$$\begin{aligned} P(\mathbf{q}, \omega_l) = & U + V(\mathbf{q}) + \frac{3}{2}U^2\chi^s(\mathbf{q}, \omega_l) \\ & - \left(\frac{1}{2}U^2 + 2UV(\mathbf{q}) + 2V(\mathbf{q})^2\right)\chi^c(\mathbf{q}, \omega_l) . \end{aligned} \quad (7)$$

The SC state is determined by the anomalous self-energy,  $\Sigma^a(\mathbf{k}, \epsilon_m)$ , defined by

$$\sum_{\mathbf{k}' \epsilon_{m'}} \int d\tau \langle T_\tau c_{\mathbf{k}' \uparrow}(\tau) c_{-\mathbf{k}' \downarrow}(0) \rangle e^{i\epsilon_{m'} \tau} P(\mathbf{k} - \mathbf{k}', \epsilon_m - \epsilon_{m'}) . \quad (8)$$

The linearized Eliashberg equation, which gives the onset of the finite value of  $\Sigma^a(\mathbf{k}, \epsilon_m)$ , is expressed as<sup>11)</sup>

$$\begin{aligned} \lambda \Sigma^a(\mathbf{k}, \epsilon_m) = & \sum_{\mathbf{k}', \epsilon_{m'}} K(\mathbf{k}, \epsilon_m; \mathbf{k}', \epsilon_{m'}) \Sigma^a(\mathbf{k}', \epsilon_{m'}) , \quad (9) \\ K(\mathbf{k}, \epsilon_m; \mathbf{k}', \epsilon_{m'}) = & -\frac{T}{N_L} P(\mathbf{k} - \mathbf{k}', \epsilon_m - \epsilon_{m'}) |G^0(\mathbf{k}', \epsilon_{m'})|^2 . \end{aligned}$$

The SC transition temperature  $T_c$  is given by the condition,  $\lambda = 1$ . Since the characteristic momentum dependence of  $P(\mathbf{q}, \omega_l)$  is essentially independent of  $\omega_l$ , and  $P(\mathbf{q}, \omega_l)$  decreases monotonously with  $|\omega_l|$ , eq. (9) is calculated by assuming a form given by

$$\Sigma^a(\mathbf{k}, \epsilon_m) = \Sigma_1^a(\epsilon_m) \Sigma_2^a(\mathbf{k}) , \quad (10)$$

where  $\Sigma_1^a(\epsilon_m)$  is evaluated by a sample average with some choices of  $\mathbf{k}$ . We solve the linearized Eliashberg equation numerically by using an iterative method where the symmetry in  $\mathbf{k}$ -space is rigorously determined without the assumption for the pairing symmetry.

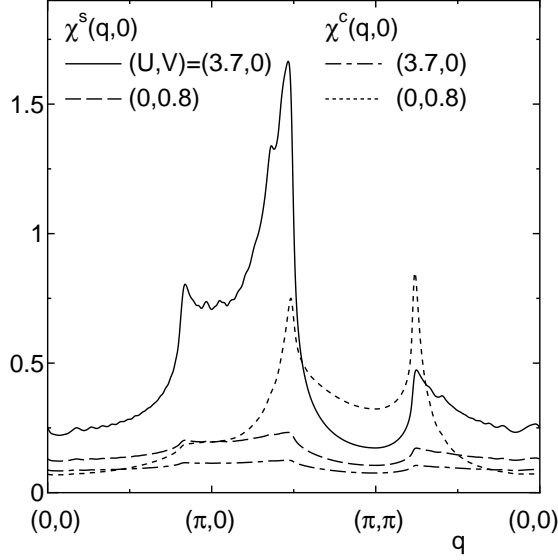


Fig. 1. Spin ( $\chi^s$ ) and charge ( $\chi^c$ ) susceptibilities for  $(U, V) = (3.7, 0), (0, 0.8)$  where  $T = 0.01$ .

We examine the role of the spin and charge fluctuations by varying  $U(\geq 0)$  and  $V(\geq 0)$ . From eqs. (4) and (5), the spin and charge susceptibilities are calculated. For  $U \neq 0$  and  $V = 0$ , the spin fluctuation is much larger than the charge fluctuation as seen from the solid line in Fig. 1. This is because the magnetic state is expected by the repulsive on site interaction leading to the enhancement of the spin fluctuation,  $\chi^s$ . The nesting condition at 3/4-filling gives rise to  $\chi^s$  being dominant in the interval region of  $(q_x, q_y) = (\pi, 0)$  and  $(\pi, \pm\pi)$ , while the peak of  $\chi^s$  at 1/2-filling appears at  $(\pi, \pi)$ . For  $V \gg U$ , the charge susceptibility,  $\chi^c$ , becomes much larger than  $\chi^s$ , since  $V$  induces CDW (or charge ordering) and then the enhancement of the charge fluctuation. In this case, as shown by the dashed line in Fig. 1, the peak of  $\chi^c$  appears as the ridge connecting two points of  $(\pi, \pi - b)$  and  $(\pi - b, \pi)$  with  $b \sim \pi/2$  in a quarter plane of  $(q_x, q_y)$ . This comes from the effect of  $V(\mathbf{q})$  in eq.(5) exhibiting a peak at  $(\pi, \pi)$  in addition to that of the nesting condition.

Based on Fig. 1, we calculate the pairing interaction,  $P(\mathbf{q}, \omega_l)$ , which is given by eq.(7). For  $U \neq 0$  and  $V = 0$ ,  $P(\mathbf{q}, 0)$  is always positive and shows the large magnitude around  $(\pi, 0)$  with the peak located between  $(\pi, 0)$  and  $(\pi, \pi)$  as seen from the solid line of Fig. 2. The  $\mathbf{q}$  dependence of  $P(\mathbf{q}, 0)$  is similar to that of  $\chi^s(\mathbf{q}, 0)$  in Fig. 1 since eq.(7) leads to  $P(\mathbf{q}, 0) \propto \chi^s(\mathbf{q}, 0)$  for  $V = 0$  and large  $\chi^s$ . However, for  $V \neq 0$ ,  $P(\mathbf{q})$  becomes different from charge and/or spin susceptibilities since the second line of eq.(7) leads to  $P(\mathbf{q})$  having the sign opposite to  $\chi^c$ . With increasing  $V/U$ ,  $P(\mathbf{q})$  begins to decrease especially in the region

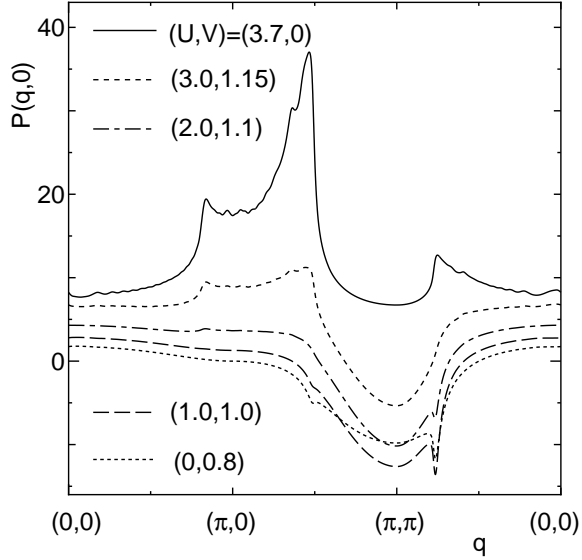


Fig. 2. Pairing interaction  $P(\mathbf{q}, 0)$  at  $T = 0.01$  for  $(U, V) = (3.7, 0)$  (solid curve),  $(3.0, 1.15)$  (short-dashed curve),  $(2.0, 1.1)$  (dot-dashed curve),  $(1.0, 1.0)$  (dashed curve) and  $(0, 0.8)$  (dotted curve).

of  $(\pi, 0)$  and  $(\pi, \pi)$  where the peak of  $P(\mathbf{q})$  is reduced noticeably and the dip around  $(\pi, \pi)$  grows leading to the attractive interaction. Thus it turns out that, with increasing  $V$ , the main part of pairing interaction becomes attractive and takes a broad dip around  $(\pi, \pi)$  but still remains repulsive in the region being away from  $(\pi, \pi)$ . Apparently, such an attractive interaction indicates the s-wave pairing but our obtained result differs from such a pairing as shown later.

The onset for the SC state is obtained by calculating eq.(9) numerically. The parameters  $U$  and  $V$  are calculated so that the maximum eigen value of  $\lambda$  may become unity with the fixed  $T$ . In Fig. 3, the solid curve corresponding to the onset of the SC state is calculated for  $T = 0.01$ . On the dashed lines, either  $\chi^s(\mathbf{q}, 0)$  or  $\chi^c(\mathbf{q}, 0)$  diverges at  $T = 0.01$ , i.e., either the incommensurate SDW or the incommensurate CDW is obtained for  $(U, V)$  in the right hand side or the upper side of the respective line. The region enclosed by the solid line, the horizontal axis and the vertical axis corresponds to the normal state. The SC state is obtained in the region enclosed by solid line and dashed two lines. The critical value of  $V$  for the onset of the SC state increases with increasing  $U$  ( $\lesssim 3$ ). This comes from the competition between the spin fluctuation and the charge fluctuation where the sign of the respective pairing interaction is opposite each other as shown in Fig. 2. Thus it is found that the pairing interaction corresponding to the onset of the SC state is mainly determined by

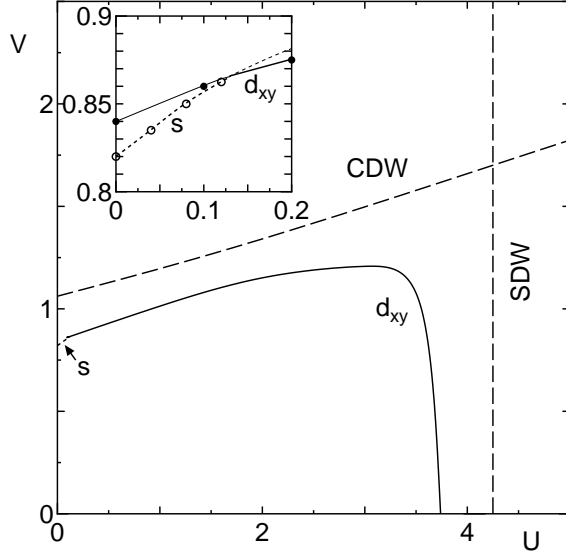


Fig. 3. Phase diagram on the plane of  $U$  and  $V$  at  $T = 0.01$  where the superconducting state (SC) is obtained in the region between the solid curve and the dashed curves. The solid curve denotes the onset for the  $d$ -wave ( $d_{xy}$ ) SC state and the dotted line denotes that for the  $s$ -wave SC state. In the inset, the detail close to  $U = 0$  is shown where solutions for both  $s$  (dotted line) and  $d_{xy}$  (solid line) exist for  $U < 0.2$ .

the charge fluctuation for  $U \lesssim 3.5$  while the spin fluctuation is dominant for  $3.5 \lesssim U \lesssim 3.7$ , i.e., close to the upper bound of  $U$ . The SC region is enlarged with decreasing temperatures since the solid curve moves toward the origin  $(0,0)$  rapidly compared with that of the dashed line.

In order to examine the symmetry of the order parameter of the SC state,  $\mathbf{k}$  dependence of the quantity  $\Sigma^a(\mathbf{k}, i\pi T)$ , is shown in Fig. 4 for three kinds of parameters. The solid line, dashed line and dotted line correspond to  $(U, V) = (3.7, 0)$ ,  $(1.0, 1.0)$  and  $(0, 0.8)$ , respectively. In the case of  $(U, V) = (3.7, 0)$  and  $(1.0, 1.0)$ , we found following two features : (1) the sign of  $\Sigma^a(\mathbf{k}, i\pi T)$  in the region of  $k_y > 0$  are different from that of  $k_y < 0$ , (2)  $\Sigma^a(\mathbf{k}, i\pi T) = 0$  on  $k_x$  and  $k_y$  axis and on the boundary of the Brillouin zone, indicating the relation,  $\Sigma^a(k_x, k_y, \epsilon_m) = -\Sigma^a(k_x, -k_y, \epsilon_m)$  and  $\Sigma^a(k_x, k_y, \epsilon_m) = -\Sigma^a(-k_x, k_y, \epsilon_m)$ . By noting the symmetry of the square lattice, this state corresponds to the  $d_{xy}$ -like symmetry. In the case of  $(0, 0.8)$ , on the other hand, the sign of  $\Sigma^a(\mathbf{k}, i\pi T)$  remains unchanged except for the region near  $(\pi, \pi)$  and  $\Sigma^a(\mathbf{k}, i\pi T)$  has a maximum near  $(0, 0)$ . Thus the dotted line of Fig. 4 indicates the  $s$ -like symmetry. In Fig. 3, such a  $s$  state is shown by the dotted line. The  $d_{xy}$  state in the case of  $(U, V) = (3.7, 0)$  is reasonable due to the repulsive interaction

located around  $\mathbf{q} = (\pi, 0)$  and seems to be consistent with that of Kondo<sup>12)</sup>, who treated the  $U$ -term perturbationally. For  $V$  being large with the moderate strength of  $U$  (dashed curve of Fig. 4), the SC state is still given by  $d_{xy}$  although the pairing interaction of Fig. 2 is almost attractive. This is understood as follows. Both  $d_{xy}$  state and  $s$  state can gain the energy from the attractive interaction close to  $(\pi, \pi)$  although the latter is slightly larger than the former due to the absence of the node. However  $d_{xy}$  state can be chosen due to the energy gain from the repulsive interaction around  $(\pi, 0)$ , which remains for the case of the dashed curve. In the case of  $(U, V) = (0, 0.8)$ , Fig. 2 shows that the repulsive interaction around  $(\pi, 0)$  becomes sufficiently small leading to  $s$  state.. The inset of Fig. 3 shows that  $d_{xy}$  state still exists as a metastable state at  $U = 0$ . It is expected that the difference of the Helmholtz free energy between  $s$  state and  $d_{xy}$  state is small for the case of small  $U$ . We note that there is no node for both  $d_{xy}$  state and  $s$  state on the Fermi surface of the present case of the 3/4-filled band.

Here, we analyze  $\Sigma^a(\mathbf{k}, i\pi T)$  by using the Fourier transformation given by

$$\Sigma^a(\mathbf{k}, i\pi T) = \sum_{mn} c_{mn} \phi_{mn}(\mathbf{k}) \quad , \quad (11)$$

with  $\phi_{mn}(\mathbf{k}) = e^{imk_x a} e^{ink_y a} / (2\pi)$ . In the case of  $(U, V) = (3.7, 0)$ , the ratio of the  $d_{xy}$ -component (i.e.,  $\phi_{d_{xy}}(\mathbf{k}) = 2 \sin k_x a \sin k_y a$ ) to other components with larger momentum is given by 1 : 0.50, while  $s$ - and  $d_{x^2-y^2}$ -component are absent. In the case of  $(U, V) = (1.0, 1.0)$ , the corresponding ratio is 1 : 0.37. For case of  $U \simeq 0$ , such a ratio remains approximately the same, and the  $s$ - and  $d_{x^2-y^2}$ -components also do not exist, whereas the  $s$ -state is located very close to that of the  $d_{xy}$ -state in the  $U$ - $V$  plane. For the case of  $(U, V) = (0, 0.8)$ , the extended  $s$  state shows three components consisting of the  $s$ -component ( $\phi_s(\mathbf{k}) = 1$ ), an extended  $s$ -component ( $\phi_{\text{ext-}s}(\mathbf{k}) = \cos k_x a + \cos k_y a$ ) and other components with larger momentum, where the respective ratio is given by 1 : 0.59 : 0.39. We note that  $\Sigma^a(\mathbf{k}, i\pi T)$  becomes negative near  $(\pi, \pi)$ .

Finally we examine the SC by varying temperature in Fig. 5. The frequency dependence in eq.(10) is discarded since such an effect becomes small with increasing temperature. With increasing  $T$  the critical values of  $V$  for onset of both the SC state and the CDW state increase at low temperatures ( $T \lesssim 0.1$ ) and at high temperatures ( $0.6 \lesssim T$ ), while the value of  $V$  decreases at the intermediate temperatures ( $0.1 \lesssim T \lesssim 0.6$ ). Such a reentrant transition of the CDW state and the SC state as the function of temperature, which resembles that of reference 8, originates in the property of eq. (5). At low temperature, the maximum of eq.(5) is given by the nesting wave vector of  $\chi^0(\mathbf{q}, \omega_l)$ , which is away from  $(\pi, \pi)$  as shown by the dotted curve of Fig. 1. With increasing temperature,  $\chi^0(\mathbf{q}, \omega_l)$  as the function of  $\mathbf{q}$  becomes broadened. The nesting wave vector begins to move toward  $(\pi, \pi)$  at  $T \simeq 0.08$  and

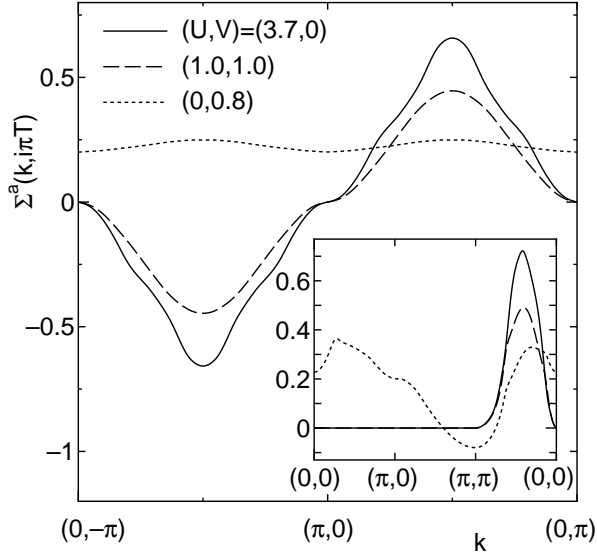


Fig. 4. Self-energy for the SC state ,  $\Sigma(k, i\pi T)$  for  $(U, V) = (3.7, 0)$ (solid line),  $(1.0, 1.0)$  (dashed line) and  $(0, 0.8)$  (dotted line) where  $T = 0.01$ . The inset shows the behavior in the quarter plane indicating that the sharp peak around  $(\pi/2, \pi/2)$  for the  $d_{xy}$  state and the broad peak around  $(0, 0)$  for  $s$  state.

also at the intermediate temperatures due to a competition of  $\chi^0(\mathbf{q}, \omega_l)$  and  $|V(\mathbf{q})|$ , which results in the increase of eq.(5). At high temperatures, eq.(5) with a maximum at  $\mathbf{q} = (\pi, \pi)$  decreases due to the further broadening of  $\chi^0(\mathbf{q}, \omega_l)$ .

In summary, we have examined the effect of nearest neighbor repulsive interaction on the SC state for the 2D extended Hubbard model with a square lattice at 3/4-filling. We found the SC state with  $d_{xy}$  symmetry for both cases of  $U$  and  $V$ , although the pairing interactions are repulsive for  $U$  and attractive for  $V$ . The spin fluctuation induced by  $U$  gives the SC state with the symmetry being the the same as that of the charge fluctuation induced by  $V$ . However the onset of the SC state needs larger magnitudes of interactions of  $U$  and  $V$  since these two fluctuations are incompatible as seen from Fig. 3. Thus it is interesting to extend the present study to the case of the SC state of organic conductors, in which exotic states may be expected due to the variety of transfer energies.

We are grateful for the financial support from a Grant-in-Aid for Scientific Research on Priority Areas of Molecular Conductors (No. 15073213 and 15073210) from the Ministry of Education, Science, Sports, and Culture, Japan and for Scientific Research from the Ministry of Education, Science, Sports and Culture, Japan (No. 14740208).



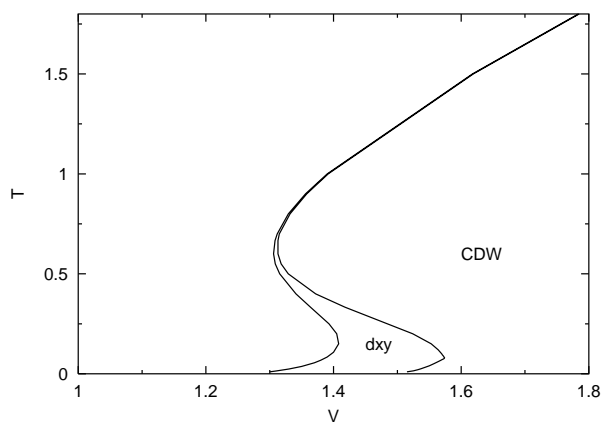


Fig. 5. Phase diagram on the plane of  $T$  and  $V$ , where  $U = 3$ .

- 
- 1) D. Jérôme and H.J. Schulz: *Adv.Phys.* **31** (1982) 299.
  - 2) H. Mori, S. Tanaka and T. Mori, *Phys. Rev. B* **57** (1998) 12023.
  - 3) C. Hotta: *J. Phys. Soc. Jpn.* **72** (2003) 840; and references therein.
  - 4) H. Taniguchi *et al.*: *J. Phys. Soc. Jpn.* **72** (2003) 468.
  - 5) N. E. Bickers and D. J. Scalapino: *Ann. Phys. (N.Y.)* **193** (1989) 206.
  - 6) H. Konntani: *Phys. Rev. B* **67** (2003) 180503(R).
  - 7) D.J. Scalapino, E.Loh, Jr. and J.E. Hirsch, *Phys. Rev. B* **35**, 6694 (1987).
  - 8) J. Merino and R. H. McKenzie *Phys. Rev. Lett.* **87**, 237002 (2001)
  - 9) G. Santoro, S. Scandolo and E. Tosatti: *Phys. Rev. B* **59** (1999) 1891.
  - 10) G. D. Mahan, *Many-Particle Physics*, 2nd ed. (Plenum Press, New York, 1990).
  - 11) *Superconductivity*, ed. by R. D. Parks, Vol. **1**, Marcel Dekker, 1969.
  - 12) J. Kondo: *J. Phys. Soc. Jpn.* **70** (2001) 808.